BMC Veterinary Research

RESEARCH

Open Access

Sheep challenged with sheep-derived type II *Mycobacterium avium* subsp. *paratuberculosis*: the first experimental model of paratuberculosis in China

Meng-Yuan Li[1†], Wei-Kang Meng[1†], Wei Ma[1†], Yu-Lin Ding[1,2], Bo Yang[3], Wei-Hong Zhao[1], Hasi Bayaer[4], Alateng Bagen[4], Rui-Bin Chen[4], Siqin Tunala[4], Rong Zhang[4], Chen-Guang Du[1], Li Zhao[1,2*] and Yong-Hong Liu[1,2*]

Abstract

Background Paratuberculosis (PTB), caused by *Mycobacterium avium* subsp. *paratuberculosis* (MAP), is difficult to diagnose in the early stages and poses substantial challenges in prevention, control, treatment, and eradication. A well-defined animal model can help identify disease markers and serve as a platform for vaccine and drug development. This study used sheep as a ruminant model for experimental MAP infection research.

Methods Nine 3-month-old lambs with negative MAP antigen and antibody were divided into three groups (control group A and inoculated groups B and C). The inoculated groups were challenged with sheep-derived type II MAP. After exposure, we recorded clinical signs, assessed fecal shedding, tested blood MAP levels, and performed fecal cultures. We also measured MAP-specific antibodies and monitored IFN-γ and IL-10 responses in vivo. At 255 days after inoculation, we performed autopsy, tissue culture, pathomorphological observation, and bacterial organ burden (BOB) testing.

Results All six sheep in groups B and C were infected, regardless of the challenge dose and exhibited emaciation; two had intermittent soft stools. Intermittent MAP shedding in feces was observed from 60 to 255 days after exposure. Typical MAP colonies formed after 4–6 weeks of fecal and tissue culture, and Ziehl–Neelsen staining showed positive results. In the groups challenged with MAP, some blood samples tested positive for MAP and MAP-specific antibodies were detected in some serum samples. IFN-γ response was significantly higher in groups B and C than that in group A from day 60 post-exposure, whereas the IL-10 response was higher than that in group A from day 120 post-exposure. In the infected groups, the ileal lesions were the most severe and were classified as grade 3 PTB granulomatous inflammation (multibacillary lesions). BOB levels varied across different tissues.

Conclusions To the best of our knowledge, this is the first experimental MAP challenge study on sheep in China. Polymerase chain reaction detection was more sensitive than MAP culture, whereas enzyme-linked immunosorbent

[†]Meng-Yuan Li, Wei-Kang Meng and Wei Ma contributed equally to this work.

*Correspondence:
Li Zhao
zhaolidky@126.com
Yong-Hong Liu
lyhdky@126.com
Full list of author information is available at the end of the article

assay was less sensitive for detecting MAP-specific antibodies. IFN-γ and IL-10 responses may serve as targets for monitoring PTB progression. The severity of ileal lesions and acid-fast bacilli grading play crucial roles in the understanding of infection dynamics. Currently, early PTB diagnosis requires a combination of multiple sample types and detection methods.

Keywords Paratuberculosis, *Mycobacterium avium* subsp. *paratuberculosis*, Sheep, Infection model

Introduction

Paratuberculosis (PTB) is a chronic infection primarily caused by *Mycobacterium avium* subsp. *paratuberculosis* (MAP) in wild and domestic ruminants. It leads to mesenteric lymphadenitis and granulomatous enteritis, followed by weight loss, diarrhea, and eventual death [1]. Animals are typically infected at a young age by ingestion of fecal-contaminated material, milk, or colostrum, either via in utero transmission or neonatal exposure [2]. The fecal–oral route is the primary mode of MAP transmission [3]. PTB is widespread across multiple countries and is considered a significant disease owing to its economic impact, effects on animal welfare, and public health concerns [4]. Moreover, MAP is a zoonotic pathogen that threatens human health [5] and enters the human food chain through contaminated meat [2], dairy products [6], and untreated water [7].

Core genome analysis has revealed two distinct MAP lineages: types S (sheep strain) and C (cattle strain or type II). Type S includes two sublineages, types I and III, and the Bison type is a distinct clade within type C; however, these are not different strain types of MAP [8–13]. Type S strains exhibit slow growth (≥ 16 weeks) and are closely associated with sheep sources, whereas type C strains grow more rapidly (4–16 weeks) and, although commonly found in cattle, have a broader host range [14]. Virulence differs between type S and C strains depending on the host species [15]. Infection of sheep with type S strains results in granulomatous lesions confined to lymphoid tissue, with no difference in lesion intensity over time. Conversely, infection with type C field strains initially causes diffuse lesions, which decrease in severity with prolonged infection duration (150–390 days) and become well-demarcated granulomas with fibrosis [16, 17].

The development of experimental infection models can help understand the dynamics of MAP infection and disease progression [3]. Previously, countries where ovine PTB posed a significant challenge have developed various experimental animal models. These models have been established in the USA (cattle [18–24], sheep [18, 25], murine [26–29], rabbit [30], and deer [25]); the UK (cattle [31, 32], sheep [33–35], and hamsters and rabbits [36]); South Korea (cattle [37] and murine [38]); Australia (sheep [39–43], cattle [44, 45], and rabbit [46]); Argentina (cattle [47–49] and murine [50, 51]); Canada (cattle [52, 53], sheep [54], murine [55, 56], and rabbit [57]); New Zealand (sheep [58, 59, 60]); Spain (sheep [17, 61–64] and rabbit [65–67]); Germany (sheep [68, 69]); Denmark (sheep [70]); Japan (murine [71]); India (cattle [72], sheep [73], and murine [74]); Iran (sheep [75]); the Netherlands (sheep [76]); and Italy (sheep [77]). To the best of our knowledge, no relevant studies have been conducted in China. This study aimed to conduct animal experiments on sheep challenged with a type II MAP strain, providing a foundation for further studies on PTB pathogenesis, early diagnosis, and control strategies.

Materials and methods

Experimental animals

Nine 3-month-old small-tail Han sheep (five males and four females) sourced from a sheep farm in Hohhot, Inner Mongolia, China, were selected for this study. The farm consistently tested negative for PTB based on multiple tests conducted in our laboratory over the past 3 years. No sheep in China were immunized with a PTB vaccine, and the farm did not administer brucellosis vaccination. Before selecting the experimental animals for this study, 20% (60/300) of the farm's sheep were randomly tested. First, blood samples were collected via the jugular vein, and fecal samples were collected from the rectum. These samples were analyzed for MAP-specific antibodies and antigens (*IS900* gene) using enzyme-linked immunosorbent assay (ELISA), DNA extraction, and polymerase chain reaction (PCR) [78, 79], following the manufacturer's protocols for ID Screen® Paratuberculosis Indirect Screening Test (ID Vet, Montpellier, France), E.Z.N.A Stool DNA Kit (Omega BioTek Inc., Norcross, GA, USA), and Premix Taq™ (TaKaRa Taq™ Version 2.0 plus dye) (TaKaRa, Beijing, China). Second, we performed serum screening for brucellosis using the plate agglutination test (GB/T 18646-2018, national standard, China), tube agglutination test (GB/T 18646-2018, national standard, China), and indirect ELISA (Laipson, Luoyang, China). Third, genomic DNA was extracted from anticoagulated blood and throat swabs using the TaKaRa MiniBEST Universal Genomic DNA Extraction Kit Ver. 5.0 (TaKaRa) and screened for *Mycobacterium tuberculosis* using a real-time PCR kit (Anheal, Beijing, China), along with fecal DNA analysis. After confirming that all tested

sheep were negative for PTB, brucellosis, and tuberculosis, nine 3-month-old lambs were selected and housed in an experimental animal facility for adaptive feeding. They were fed lamb feed and lucerne at regular, quantitative intervals each day and were subsequently dewormed. One week later, they were retested for PTB, brucellosis, and tuberculosis. After confirming the negative results, further animal experiments were initiated. Three groups of sheep were housed under identical conditions in isolation. No experimental animals received antibiotics or immunosuppressive drugs.

MAP preparation and animal grouping for the challenge

MAP was cultivated, identified, and stored at −80°C in our laboratory. A third-passage culture of a type II MAP strain (MAP-NM5), originally isolated from ovine intestines, was used as the inoculum. The seed stock was transferred to 7H9 liquid culture medium (Middlebrook, Becton Dickinson, NJ, USA), supplemented with glycerin (Merck, Darmstadt, Germany), Middlebrook OADC (Middlebrook), and Ferric Mycobactin J (MYCO, ID Vet). The culture was incubated at 37°C with continuous shaking at 160 rpm for 67 days. Optical density at 600 nm (OD_{600}) was measured using an ELISA reader (BioTek Instruments, Inc., VT, USA), and culturing was stopped once the bacterial count reached 10^7 CFU/mL. Subsequently, experimental animals were prepared for inoculation. Batch suspensions were confirmed to contain acid-fast bacilli (AFB) via Ziehl–Neelsen (ZN) staining, and the presence of MAP was verified using PCR, following the aforementioned method.

Nine lambs were randomly assigned to three groups for the MAP challenge: control group A ($n = 3$; males: 2, female: 1; numbered 1–3), inoculated group B ($n = 3$; males: 3; numbered 4–6), and inoculated group C ($n = 3$; females: 3; numbered 7–9). For 4 consecutive days, the inoculated groups were orally inoculated with MAP. Each sheep in group C received approximately 2.57×10^9 CFU of live bacteria, whereas each sheep in group B received approximately 9.2×10^8 CFU. Control group A was administered an equivalent volume of 7H9 liquid culture medium. Post-exposure time was defined as the time elapsed from the date of the first MAP inoculation.

Post-exposure detection

Following the MAP challenge, the clinical symptoms of all experimental animals were monitored daily. Fecal samples were collected from the rectum of each sheep daily during 1–3 days post-exposure. Due to COVID-19 management policies in China, sheep no. 3 from control group A died on day 27 post-exposure, and led to a modification of the sampling schedule. From day 60 post-exposure, fecal samples were collected from the rectum and blood was drawn from the jugular vein at 15-day intervals for serum separation. The methods used for DNA extraction and MAP detection in whole blood and fecal samples as well as for MAP-specific antibody detection in serum were the same as those used during experimental animal selection. Serum interferon-γ (IFN-γ) and interleukin-10 (IL-10) levels were measured using the Sheep IFN-γ ELISA Kit (BlueGene Biotech, Shanghai, China) and Sheep IL-10 ELISA Kit (BlueGene Biotech), according to the manufacturer's protocols.

The experiment was terminated at 255 days post-exposure, after which the lambs were euthanized and necropsied. Gross lesions examined across various organs and tissue samples, including intestinal and mesenteric lymph nodes, were collected. For histopathological examination, tissue samples were fixed in 10% neutral formalin, embedded in paraffin, sectioned, and stained using hematoxylin–eosin (HE) and ZN staining. The tissue used for electron microscopy was fixed in 2.5% glutaraldehyde, and ultra-thin sections were prepared by Saixin Natural Gene Technology (Beijing, China). For bacterial organ burden (BOB) detection, DNA was extracted using the TaKaRa MiniBEST Universal Genomic DNA Extraction Kit Ver. 5.0 (TaKaRa). Fluorescent quantitative PCR was performed using TB Green® Premix Ex Taq™ II (Tli RNaseH Plus) (TaKaRa). Primers were F1 (AATGACGGTTACGGAGGTGGT) and R1 (GCAGTA ATGGTCGGCCTTAC). The BOB results were analyzed using one-way analysis of variance with 95% confidence intervals. Two-tailed p-values <0.05 were considered statistically significant. Data were visualized using Prism 8 (GraphPad, USA).

At each experimental stage, fecal samples were collected, and tissue samples were obtained during necropsy for MAP culture [68]. Following bacterial culture, DNA was extracted using the TaKaRa MiniBEST Bacteria Genomic DNA Extraction Kit Ver. 3.0 (TaKaRa) following the manufacturer's instructions. PCR was performed, and all PCR-positive products were sequenced by Sangon Biotech (Shanghai, China). The sequencing results were compared with those of the inoculated MAP strain (MAP-NM5). Additionally, colony smears were prepared and subjected to ZN staining.

Results

Clinical signs

Compared with group A, sheep in groups B and C exhibited slower growth rates. At the end of the experiment, the animals were significantly emaciated with dry and dull fur, particularly sheep no. 9. Additionally, sheep nos. 5 and 7 experienced intermittent fecal softening, wherein feces failed to form granules and instead turned into lumps.

Fecal shedding

Overall, 139 fecal samples were collected post-exposure (17 time points × 8 surviving sheep + 3 accidental deaths of sheep). PCR analysis confirmed that all group A fecal samples were negative for MAP, whereas those from groups B and C at 1–3 days post-exposure were positive. From 60 days post-exposure, fecal samples were collected at 14 regular intervals, which revealed intermittent MAP shedding. Fecal shedding detection rates in sheep nos. 4–9 were 42.86% (6/14), 57.14% (8/14), 21.43% (3/14), 64.29% (9/14), 57.14% (8/14), and 64.29% (9/14), respectively. Fecal shedding was first detected at 60 days post-exposure (Table 1).

Fecal and tissue culture

A total of 14 samples (including 8 MAP-positive samples based on PCR) were collected from sheep nos. 5 and 9 at 60, 75, 90, 105, 120, 135, and 150 days post-exposure, along with 16 tissue samples (ileum and mesenteric lymph nodes) from eight sheep. After 4–16 weeks of cultivation, MAP colonies were observed in four fecal samples: sheep no. 9 at 75 days (culture time: 4 weeks), 105 days (6 weeks), and 150 days (6 weeks) post-exposure and sheep no. 5 at 120 days post-exposure (6 weeks). Additionally, seven tissue samples tested positive: the ileum of sheep no. 4 (4 weeks), the ileum of sheep nos. 5, 7, 8, and 9 (6 weeks), and the mesenteric lymph nodes of sheep nos. 8 and 9 (6 weeks). The colonies appeared nipple-shaped, with irregular edges, a smooth surface, and a creamy or pale yellow color. ZN staining confirmed a short rod-shaped AFB with consistent morphology and size (Fig. 1). PCR amplification of the colonies revealed positive results, and the sequencing results matched the challenge strain (MAP-NM5) gene sequence.

MAP detection in whole blood

Overall, 112 blood samples (14 time points × 8 sheep) were collected post-exposure. All group A samples were PCR-negative for MAP, whereas some samples in groups B and C tested PCR-positive for MAP. MAP was detected in sheep no. 4 (once at 105 days post-exposure), sheep no. 5 (once at 60 days post-exposure), sheep no. 6 (twice at 105 and 180 days post-exposure), sheep no. 7 (four times at 105, 135, 150, and 165 days post-exposure), sheep no. 8 (thrice at 105, 120, and 135 days post-exposure), and sheep no. 9 (twice at 105 and 120 days post-exposure) (Table 1).

Table 1 MAP-specific antibodies in serum and MAP antigen detection in feces and blood

Days post inoculation (d)	Fecal samples						Blood samples						Serum samples					
	Group B			Group C			Group B			Group C			Group B			Group C		
	4	5	6	7	8	9	4	5	6	7	8	9	4	5	6	7	8	9
1	+	+	+	+	+	+	*	*	*	*	*	*	*	*	*	*	*	*
2	+	+	+	+	+	+	*	*	*	*	*	*	*	*	*	*	*	*
3	+	+	+	+	+	+	*	*	*	*	*	*	*	*	*	*	*	*
60	–	–	–	+	–	–	–	+	–	–	–	–	–	–	–	–	–	–
75	+	–	–	–	–	+	–	–	–	–	–	–	–	–	–	–	–	+
90	–	+	–	+	+	–	–	–	–	–	–	–	–	–	–	+	–	–
105	+	–	+	+	–	+	+	–	+	+	+	+	–	–	–	–	–	–
120	–	+	–	+	+	+	–	–	–	–	+	+	–	–	–	–	–	–
135	+	+	–	–	+	–	–	–	–	+	+	–	–	–	–	–	–	–
150	–	+	+	+	+	+	–	–	–	+	–	–	–	–	–	+	–	–
165	–	+	–	+	–	+	–	–	–	+	–	–	–	–	–	–	–	–
180	–	+	–	–	–	–	–	–	+	–	–	–	–	–	–	–	–	+
195	+	+	–	+	+	+	–	–	–	–	–	–	–	–	–	–	–	+
210	–	–	–	–	+	+	–	–	–	–	–	–	–	–	–	–	–	+
225	+	+	–	–	+	+	–	–	–	–	–	–	–	–	–	–	–	+
240	+	–	+	+	+	+	–	–	–	–	–	–	–	–	–	–	–	+
255	–	–	–	+	–	–	–	–	–	–	–	–	–	–	–	–	–	+
Positive rate (%)	42.86	57.14	21.43	64.29	57.14	64.29	7.14	7.14	14.29	28.57	21.43	14.29	0	0	0	14.29	0	50

"+" represents positive

"–" represents negative

"*" represents not sampled

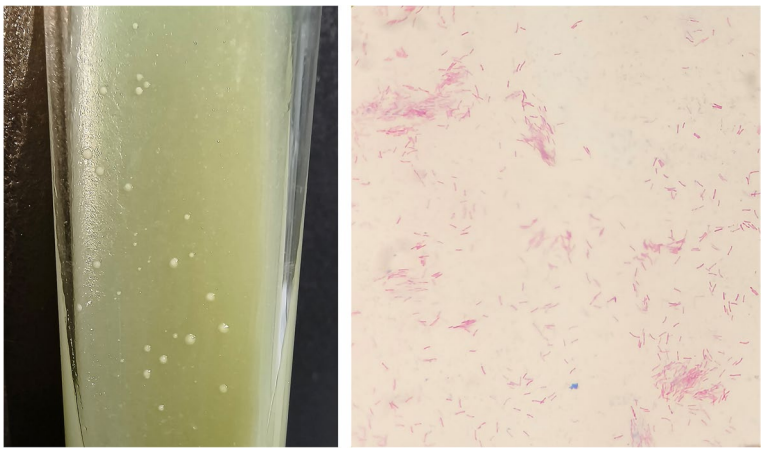

Fig. 1 MAP cultivation and identification (The left panel shows smooth growth of papillary MAP colonies on the surface of culture medium, and the right panel shows Ziehl–Neelsen acid-fast staining of a bacterial smear showing short, rod-shaped acid-fast bacilli (AFB) with uniform morphology and size)

Antibody response

Among the 112 serum samples, only sheep no. 7 and 9 tested positive for MAP-specific antibodies: sheep no. 7 tested positive twice (at 90 and 150 days post-exposure) and sheep no. 9 tested positive seven times (75, 180, 195, 210, 225, 240, and 255 days post-exposure) (Table 1).

IFN-γ and IL-10 response

Among the 112 serum samples, group A exhibited extremely low cytokine concentrations, with no significant differences in IFN-γ or IL-10 levels. Conversely, groups B and C showed a significantly higher IFN-γ response than group A from 60 days post-exposure, peaking at 105–135 days, followed by a gradual decline from 150 days and stabilization at a relatively high level between 180 and 255 days, remaining higher than group A. The IL-10 response in groups B and C began increasing compared with that of group A from 120 days post-exposure and showed a continuous upward trend. The IL-10 response of sheep no. 5 was lower than that of the other sheep in groups B and C starting from 150 days post-exposure but was still higher than that of group A (Fig. 2). There were no significant differences in cytokine responses between groups B and C.

Pathological changes

Gross pathology

Group A exhibited no obvious gross lesions. In groups B and C, sheep exhibited pale visible mucosa, light and sparse blood, small amounts of edematous fluid in the chest and abdominal cavities, muscle thinning, and adipose tissue atrophy with a pale yellow, jelly-like appearance. Additionally, sheep nos. 5 and 7 showed significant edema in the lower jaw. Prominent gross lesions were observed in the intestine and mesenteric lymph nodes.

Lesions in the small intestine, primarily affecting the jejunum and ileum, were characterized by marked intestinal contraction, thickened intestinal walls, and

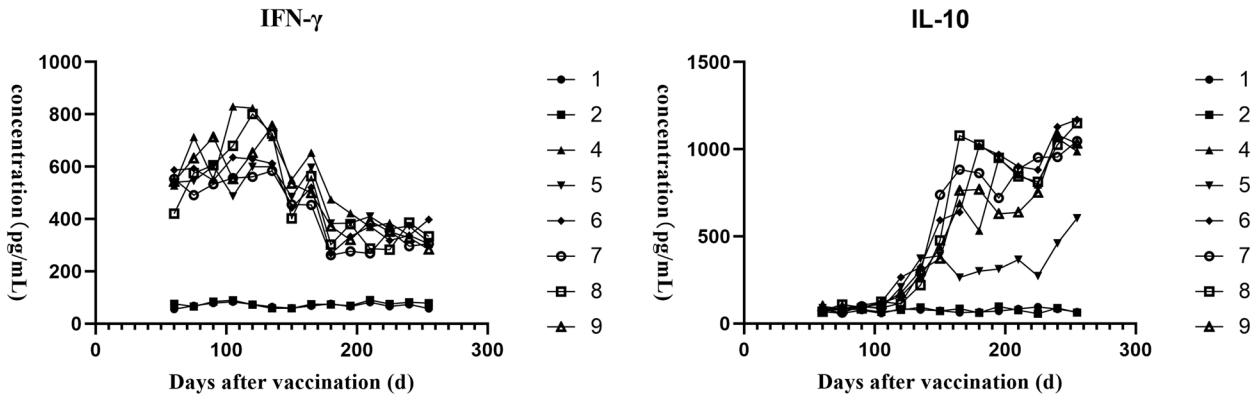

Fig. 2 IFN-γ and IL-10 response (The left and right panels show IFN-γ and IL-10 responses, respectively, in sheep serum)

diffuse mucosal folds, giving the intestine a "gyrus-like" appearance. Large intestinal lesions, mainly observed in the cecum and proximal colon, were relatively mild and resembled those in the small intestine. Mild mesenteric lymph node enlargement was noted, with uneven, moist cross-sections that appeared pale or grayish-yellow. Additionally, some mesenteric lymph nodes contained gray–white calcifications of varying sizes on the cut surface (Fig. 3).

Histopathology

Group A sheep exhibited no significant histopathological changes, whereas sheep in groups B and C showed similar lesions, which were mainly concentrated in the intestinal and mesenteric lymph nodes. In the duodenum, cecum, and colon, scattered individual cells or clusters of lymphocytes, macrophages, epithelioid macrophages, and plasma cells were present in the lamina propria, with a few epithelioid macrophages containing sparse AFB in their cytoplasm (Fig. 4). The jejunal villi were blunt and fused, with extensive infiltration of lymphocytes and epithelioid macrophages in the lamina propria, along with the presence of focal granulomas. Most epithelioid macrophages contained a large abundant AFB (Fig. 5). Multifocal granulomatous lesions were visible in the jejunal lamina propria of sheep no. 5. The ileum exhibited intestinal villi atrophy and fusion, with multifocal or diffuse granulomatous lesions surrounded by a large number of lymphocytes in the lamina propria (Fig. 6a). Multinucleated giant cells were observed within the granulomas (Fig. 6b), and a large number of epithelioid macrophages contained a significant amount of AFB (Fig. 6c). In addition, focal fibrotic granulomatous lesions were present in the ileal submucosal layer of sheep no. 5 (Fig. 6d). In the mesenteric lymph nodes, connective tissue hyperplasia was observed in the capsule (Fig. 7a), along with multifocal granulomatous lesions (Fig. 7b) containing numerous macrophages, epithelioid macrophages, and multinucleated giant cells in the cortical region (Fig. 7c). Clusters of AFB were also observed in the cytoplasm of macrophages and epithelioid macrophages in the medulla (Fig. 7d). Liver cell granular degeneration and necrosis were observed in sheep nos. 8 and 9, whereas focal granulomas were observed in the liver parenchyma of sheep nos. 5, 8, and 9 (Fig. 8). Additionally, AFB were present in the macrophages of the retropharyngeal and superficial cervical lymph nodes.

Ultrastructural pathology

Numerous macrophages were observed in the intestinal and mesenteric lymph nodes, with an increased number of phagolysosomes within the cytoplasm.

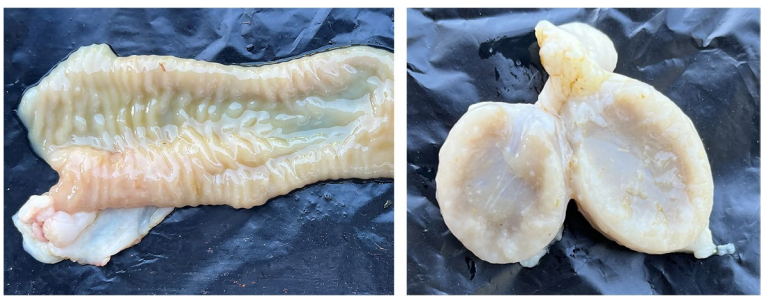

Fig. 3 Gross pathology (The left panel shows ileal mucosa exhibiting diffuse folds resembling a gyrus, and the right panel shows mesenteric lymph nodes with an uneven sectional appearance and gray–white calcifications of varying sizes)

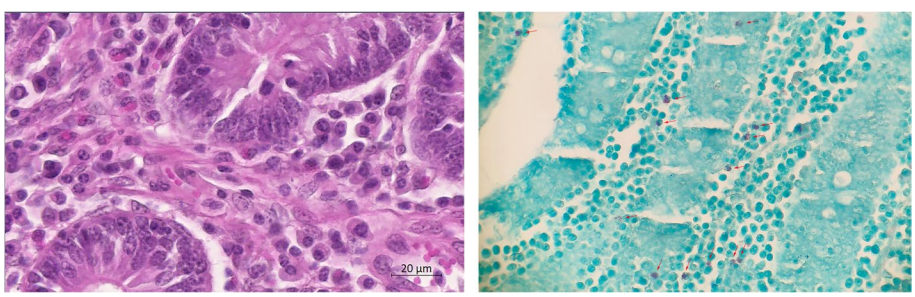

Fig. 4 Histopathology of the duodenum (Left: Hematoxylin–eosin [HE] staining of the duodenal lamina propria showing infiltration of lymphocytes, macrophages, epithelioid macrophages, and plasma cells; Right: Ziehl–Neelsen acid-fast staining of the duodenal lamina propria showing epithelioid macrophages with sparse intracellular acid-fast bacilli [AFB] (red arrow))

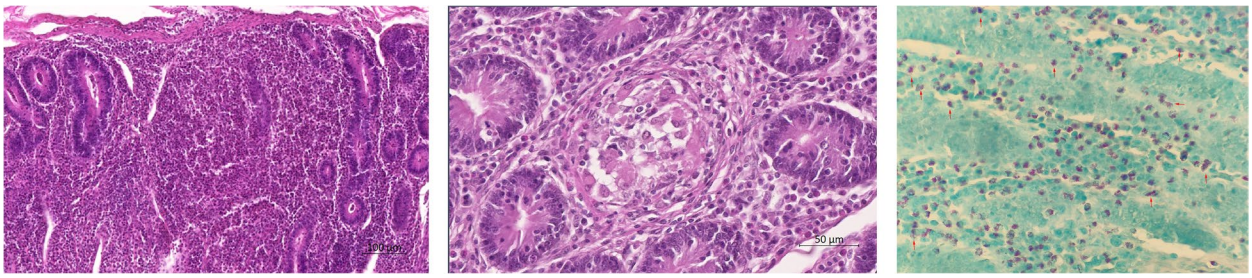

Fig. 5 Histopathology of the jejunum (Left: HE staining of the jejunal submucosa showing infiltration of numerous lymphocytes and epithelioid macrophages; Middle: HE staining of the jejunal lamina propria of sheep no. 5 showing granuloma formation with fibrosis; Right: Ziehl–Neelsen acid-fast staining of the jejunal lamina propria showing epithelioid macrophages containing abundant intracellular acid-fast bacilli [AFB] (red arrow))

Mitochondrial swelling and rough endoplasmic reticulum expansion into vesicles were noted. Additionally, both intact and partially degraded MAP were observed in the cytoplasm of macrophages (Fig. 9).

BOB

Significant differences in BOB levels were observed between the liver and spleen ($p = 0.0149$) and between the liver and kidneys ($p = 0.0481$), whereas no significant difference in BOB levels was observed between the spleen and kidneys ($p = 0.8208$). The tonsils exhibited a significantly higher BOB levels than the adrenal glands ($p = 0.0047$) and porta hepatis lymph nodes ($p = 0.0059$). The mesenteric lymph nodes had a significantly higher BOB than the adrenal glands ($p = 0.0003$) and porta hepatis lymph nodes ($p = 0.0004$). There were no significant differences in BOB levels between the tonsils and mesenteric lymph nodes ($p = 0.6470$) or between the adrenal glands and hepatic hilum lymph nodes ($p = 0.9996$).

In the intestinal tissues from the duodenum to the rectum, the jejunum, ileum, and cecum exhibited higher BOB levels, with the ileum having the highest BOB (significantly higher than that of the duodenum, cecum, colon, and rectum [$p < 0.0001$]; significantly higher than that of the jejunum [$p = 0.0019$]), while the BOB of the rectum was the lowest (significantly lower than that of the jejunum [$p = 0.0002$]). Furthermore, the jejunum had a significantly higher BOB than the colon ($p = 0.0019$). Significant differences in BOB levels were also observed between the duodenum and jejunum ($p = 0.0318$) and between the cecum and rectum ($p = 0.0105$), whereas no significant differences were observed among the remaining intestinal tissues. All four stomach compartments tested positive for MAP; however, BOB levels were very low, with no significant differences among the compartments.

Discussion

The World Organization for Animal Health has recognized PTB as a major global animal health concern [80] and classified it as a "neglected disease" [81]. No country has been declared free of MAP [82]. However, underreporting and underestimation of prevalence remain widespread, and many countries lack formal control plans [4]. Effective PTB control requires critical progress in diagnosis and vaccine development and a deeper understanding of host–pathogen interactions [83]. PTB experimental infection models are crucial for studying epidemiology, economic impact, infection dynamics, and control strategies [3]. In Chinese terminology, the relationship between the pathogen and animal model can be likened to the spear and shield, allowing exploration of both pathogen virulence (spear sharpness) and host resistance (shield strength). Small ruminants are natural hosts for MAP, with sheep serving as an ideal animal model for PTB, which has several advantages, including genetic consistency, low cost, and ease of experimental operation [84]. Historically, sheep has been a convenient ruminant model in MAP infection research [3]. In this study, the combination of MAP colonization, intestinal and mesenteric lymph node granuloma, multibacillary lesions, and fecal shedding satisfied the criteria for developing a successful sheep infection MAP model [3].

Clinical signs

In the present study, MAP-infected sheep exhibited clinical changes, including malnutrition, indicating that MAP negatively affects sheep health. However, only sheep nos. 5 and 7 showed intermittent fecal softening, without the typical symptoms of PTB-associated diarrhea [3]. In small ruminants, the symptoms of PTB are subtler, with a long incubation period in sheep. Clinical symptoms typically appear between 2 and 4 years of age and are primarily manifesting as progressive emaciation [85]. The post-exposure results indicate different stages

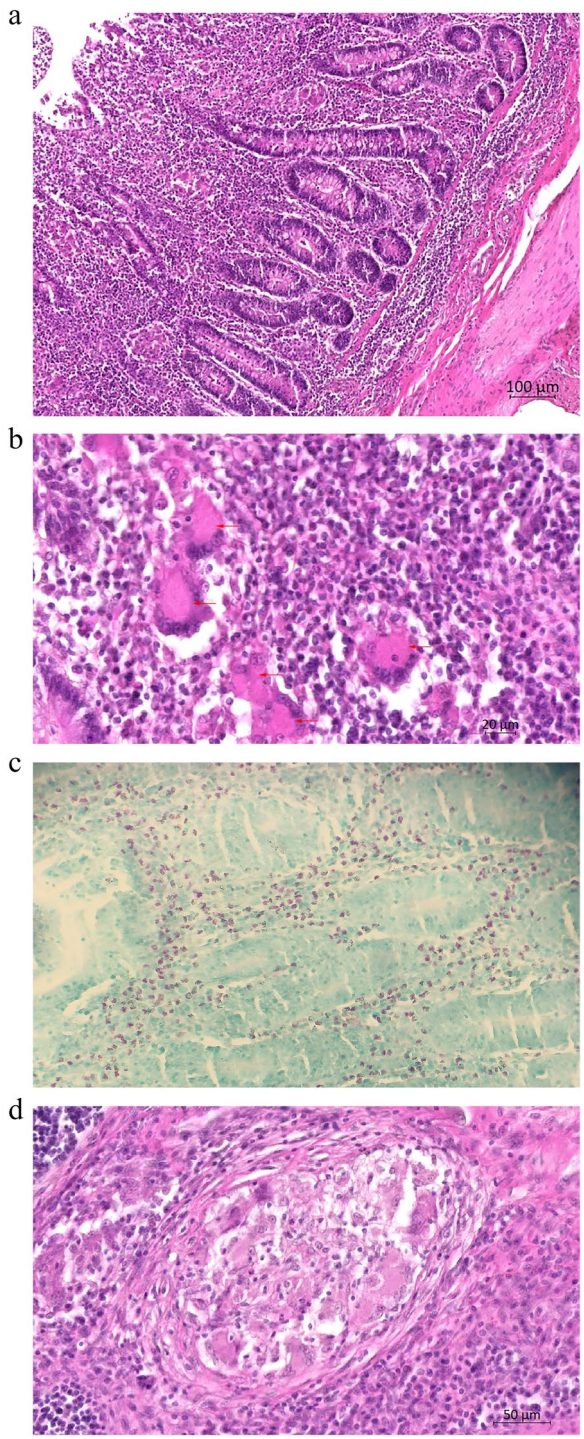

Fig. 6 Histopathology of the ileum (a: HE staining of the ileal lamina propria showing multifocal granulomatous lesions with visible submucosal layers; b: HE staining of the ileal lamina propria showing diffuse granulomatous lesions with lymphocytes, epithelioid macrophages, and multinucleated giant cells (red arrow); c: Ziehl–Neelsen acid-fast staining of the ileal lamina propria showing numerous epithelioid macrophages with abundant intracellular AFB; d: HE staining of the ileal submucosa of sheep no. 5 showing focal fibrotic granulomatous lesions)

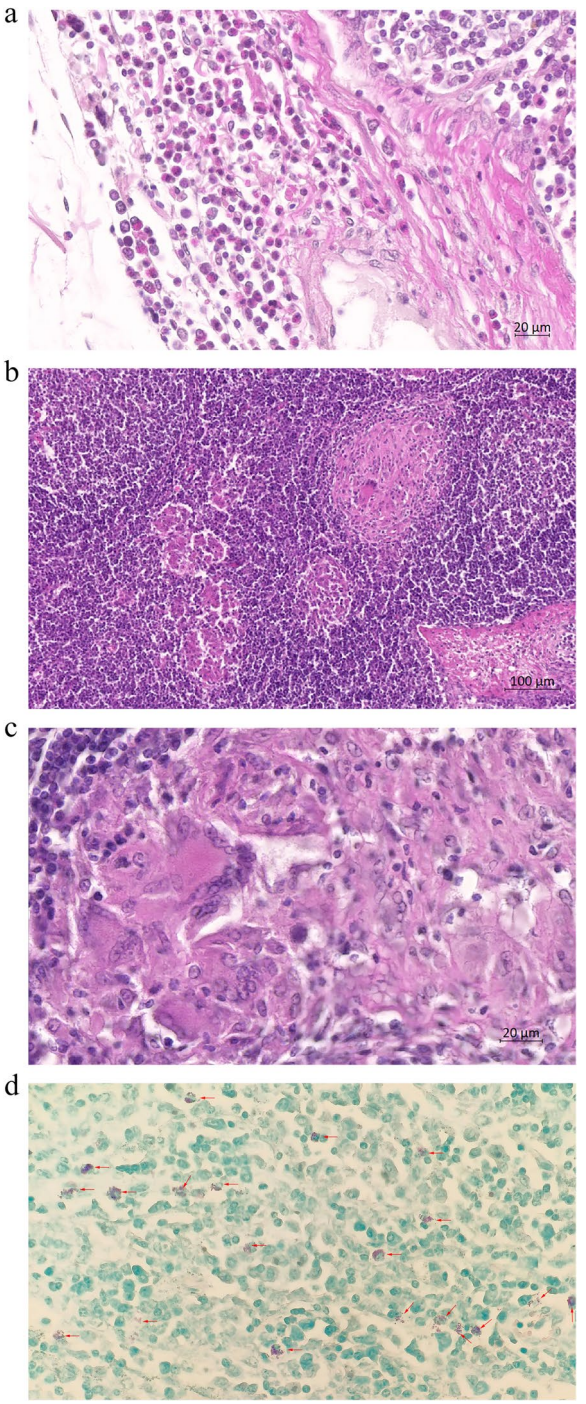

Fig. 7 Histopathology of mesenteric lymph nodes (a: HE staining of mesenteric lymph nodes showing infiltration of lymphocytes, macrophages, and epithelioid macrophages in the subcapsular sinus and paracortex; b: HE staining of the mesenteric lymph node cortex showing multifocal granulomatous lesions; c: HE staining of mesenteric lymph nodes showing granulomas primarily composed of epithelioid macrophages and multinucleated giant cells; d: Ziehl–Neelsen acid-fast staining of mesenteric lymph nodes showing AFB (red arrow) within the cytoplasm of medullary and epithelioid macrophages)

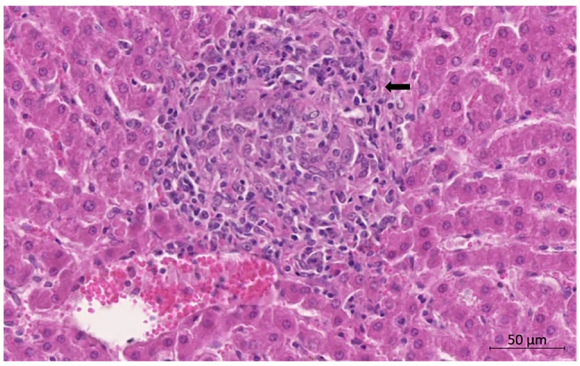

Fig. 8 HE staining of liver parenchyma showing focal granulomas (arrow) composed of lymphocytes, macrophages, and epithelioid macrophages

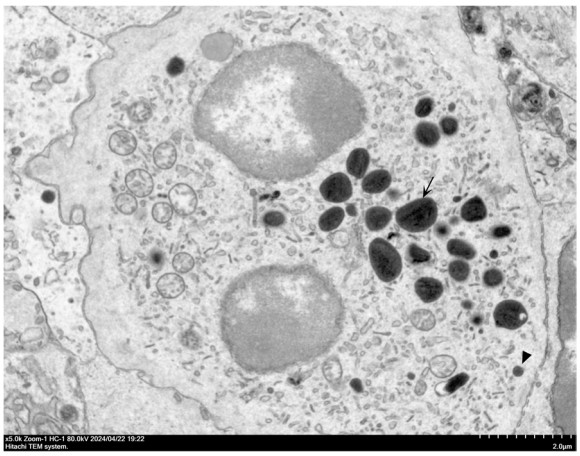

Fig. 9 Transmission electron micrograph. Mesenteric lymph node. Mesenteric lymph node. Engulfed bacteria (black arrow) and damaged or degraded bacteria (black arrowhead) in multinucleated giant cell

of MAP infection, including latent infection, active infection, and clinical affection [3]. Based on the results of various tests conducted on sheep after the MAP challenge at 255 days in this study, the infection was classified as active. Although the affected sheep did not exhibit classic PTB symptoms, significant pathological damage was observed in some individuals, indicating potential progression toward clinical disease and implications for infection dynamics. Additionally, PTB outcomes following exposure are influenced by host-related factors (age at exposure and breed) and pathogen-related factors (MAP dose, strain type, and inoculum used in experimental infections) [3, 86].

Fecal shedding

In this study, fecal tests conducted 1–3 days after exposure detected MAP, indicating pass-through rather than active shedding. From 60 days post-exposure, intermittent MAP-positive fecal samples indicated active shedding and true infection. These findings align with those of previous studies in that pass-through occurs within 10 days of oral MAP ingestion [87], and 14 days post-inoculation fecal shedding indicates the proliferation of host MAPs [88]. Histopathological examination of the ileum revealed multibacillary lesions despite the absence of persistent fecal shedding. Consistent with previous reports, transient shedding began 2 months after inoculation [89]. A long-term study (3–4.5 years) documented intermittent shedding in 10 sheep during the first year [90]. Additionally, in a previous study, fecal samples collected 42 days after exposure in a caprine model were positive for MAP [68]. However, as the earliest sampling in this study occurred at 60 days post-exposure, determining the earliest fecal shedding time was not possible. Fecal shedding indicates that infected animals act as risk factors, repeatedly exposing susceptible animals to MAP, thereby influencing infection dynamics. The progression of this infection may lead to continuous daily shedding, thereby becoming a significant risk factor in infection dynamics. Alternatively, shedding may cease permanently within 16 months post-exposure [3]. Because the present study had a 255-day challenge period, it was difficult to predict the possibility of permanent shedding and its cessation.

Although MAP culture identification is considered the "gold standard" for PTB diagnosis [91], PCR detection in this study demonstrated higher sensitivity than MAP culture results. Previous studies have also reported transient MAP shedding in the feces of most sheep within the first few months post-inoculation [92], and quantitative PCR—a more sensitive method—can effectively distinguish between low and high shedders [90]. The low sensitivity of fecal culture may be attributed to intermittent shedding in the early stages of infection, wherein MAP levels decrease beyond the detection limit. Additionally, antibiotic treatment of fecal samples before culture can inhibit MAP growth [93]. Tissue PCR is more sensitive than tissue culture, particularly for latent infection [94, 95].

MAP detection in whole blood

In this study, intermittent or short-term sustained MAP positivity in blood was observed via PCR in sheep no. 5 (60 days post-exposure), sheep no. 4 (105 days post-exposure), sheep no. 6 (105 and 180 days post-exposure), sheep no. 9 (105 and 120 days post-exposure), sheep no. 8 (105, 120, and 135 days post-exposure), and sheep no. 7 (105, 135, 150, and 165 days post-exposure), primarily during the early post-exposure stages. MAP has been detected in the blood of infected cattle and sheep via PCR and in the blood of patients with Crohn's disease via

culture and PCR [88]. Additionally, bacteremia has been reported in goats, deer, and other species [88]. Findings from this study, combined with histopathological lesions in the intestine and liver, indicate that orally ingested MAP may enter the intestine, travel through the portal vein to the liver, and subsequently enter the bloodstream via the posterior vena cava, leading to low-level transient bacteremia.

Antibody response

In this study, only sheep no. 7 (90 and 150 days post-exposure) and sheep no. 9 (75, 180, 195, 210, 225, 240, and 255 days post-exposure) exhibited intermittent or transiently continuous positive antibody responses. Compared with MAP culture, ELISA is a cost-effective alternative for PTB detection [96], with a specificity of 48%–92% and a sensitivity of 50%–70% for PTB detection [97]. Previous studies have also reported significant variability in antibody responses. For instance, one study found that over one-third of sheep tested positive after 8 weeks post-inoculation, with 41%–55% positivity during the study period [60]. The first pure-culture MAP sheep infection model detected no antibody response after 4 months post-exposure, and only 10% of sheep tested positive by 8 months post-exposure [40]. Variability in ELISA results for anti-MAP antibody detection can be attributed to the delayed interval between the humoral immune response in infected sheep, differences in antigen composition across commercial ELISA kits used in different countries, and cross reactivity with other mycobacteria, which may compromise the specificity of serological testing [60].

IFN-γ and IL-10 response

A longitudinal analysis of immune responses throughout PTB progression is crucial for understanding disease pathogenesis, diagnostic potential, and biomarker identification [45]. In this study, the exposure groups had higher IFN-γ levels than the control group from 60 days post-exposure, which peaked between 105 and 135 days post-exposure, began to decline at 150 days, and remained relatively stable from 180 to 255 days post-exposure. At 120 days post-exposure, the IL-10 response was higher than that in the control group and showed a continuous upward trend. This finding is consistent with that of de Silva et al. [98], who reported that IL-10 levels increased at 4 months post-inoculation in sheep. Coussens et al. [99] reported elevated IL-10 gene expression in peripheral blood mononuclear cells from subclinical-stage cows stimulated with MAP in vitro. IL-10 expression significantly differs between sheep with paucibacillary and those with multibacillary disease [100]. The switching between Th1 and Th2 responses is a complex process that may be triggered by MAP exposure dose, macrophage bursting size, T-cell exhaustion, and other host-level metabolic triggers [3]. Additionally, infection with type C MAP strains has been reported to elicit a stronger IFN-γ response [3].

Pathological changes

In this study, gross lesions included intestinal mucosa thickening, mesenteric lymph node enlargement, and lymphangiectasia, consistent with the findings reported by Verin et al. [101]. These lesions hinder the intestinal absorption of water and nutrients, thereby leading to diarrhea, emaciation, and cachexia in affected animals [102]. This study concluded 255 days post-exposure, and the sheep did not exhibit diarrhea and cachexia; however, histopathological and ultrastructural lesions reflected severe damage to tissue function.

The primary focus in the PTB examination was granulomatous inflammation and AFB presence. In this study, sheep in groups B and C exhibited similar lesions, with ileal lesions being the most severe. Multifocal granulomatous lesions and multinucleated giant cells were observed, and most epithelioid macrophages contained a large amount of AFB. Based on the earliest PTB histopathological classification system [103] and the granulomatous inflammation grading system for ileal and mesenteric lymph node lesions [104], lesion severity is categorized as follows: grade 1, few or clustered epithelioid macrophages and rare AFB; grade 2, focal granuloma with only a few macrophages containing small amounts of AFB; grade 3, multifocal granulomatous inflammation, wherein most macrophages contain abundant AFB; and grade 4; diffuse granulomatous inflammation, wherein most macrophages are expanded due to AFB accumulation. According to the aforementioned lesion grading criteria, it was classified as grade 3. A previous study showed that an MAP challenge dose of 10^3–10^6 CFU induces focal lesions, whereas a higher dose of 10^8–10^9 CFU results in extensive and severe lesions [3]. In this study, the inoculation dose corresponded with the severity of observed lesions. Sheep typically develop lesions within 6–12 months after positive culture detection [104]. In this study, MAP culture yielded positive results at 75 days post-exposure, which was in agreement with the lesions observed at the 255-day post-exposure necropsy. Additionally, the presence of intestinal histopathological lesions appears to be a strong indicator of MAP shedding and vice versa [3].

The results of this study demonstrated that the ileal BOB was the highest, and acid-fast staining revealed that the ileal lesions were multibacillary lesions. Previous studies have reported that MAP infection initially establishes in the lymphoid tissue of the small intestine, which may cause segmental lesions at multiple locations and

spread to the lamina propria and local lymph nodes [73]. The ileum may be the first site of MAP invasion and colonization [20]. MAP antigen exposure triggers an inflammatory response in the intestinal and mesenteric lymph nodes, resulting in granuloma formation. Granulomatous inflammation with MAP-containing macrophage infiltration occurs in the ileum [105]. In naturally infected sheep, lesions are primarily found in the jejunum, ileum, and mesenteric lymph nodes [94, 104]. Consistent with the findings of this study, a previous study reported that MAP is more abundant in the intestinal mucosa than in the mesenteric lymph nodes [104]. Therefore, active infection, particularly in the early stages, can be determined by histopathological examination of the ileum or jejunum rather than mesenteric lymph nodes. Moreover, previous studies have clearly stated that histological lesions and their grading are good indicators of active infection and affection [3].

In this study, multinucleated giant cells were observed in the ileal and mesenteric lymph nodes of sheep challenged with type II MAP. The presence of Langhans-type giant cells is reported to be a typical feature of C strain–induced lymph node granuloma [17]. Multinucleated giant cells are mainly observed in severe cases, and the more numerous they are, the higher is their effect on inflammation [106]. These cells can clear cellular debris and free MAP antigens at the site of lesions [107]. Additionally, sheep no. 5 exhibited focal fibrotic granulomatous lesions in the ileal submucosal layer, indicative of a "regressive"-type granuloma change. This indicates a potential shift toward lesion regression, disease recovery, and MAP clearance [3].

Notably, the tonsils exhibited a higher BOB than the adrenal glands and porta hepatis lymph nodes. In addition to the small intestine, the tonsils are reported to be a common site of MAP invasion [23]. Moreover, in the present study, liver focal granulomas and intestinal and mesenteric lymph node–associated tissues had a certain degree of BOB, and posterior pharyngeal and superficial cervical lymph nodes had AFB. These findings are consistent with those of a previous study reporting persistence of MAP in extraintestinal tissues, as observed in goats 12 months post-inoculation [69]. The outcomes of MAP challenge depend on various biological factors, including the MAP strain, inoculation dose, route of exposure, sheep breed, age at infection, culture conditions (subcultured organisms vs. tissue homogenates), and host susceptibility. In conclusion, early diagnosis of PTB should be based on actual scenarios by combining multiple sample types and testing methods.

Abbreviations

PTB	Paratuberculosis
MAP	*Mycobacterium avium* Subsp. *Paratuberculosis*
AFB	Acid-fast bacilli
IFN-γ	Gamma interferon
IL-10	Interleukin-10
PCR	Polymerase chain reaction
ELISA	Enzyme linking immunosorbent assay
HE	Haematoxylin and eosin staining
ZN	Ziehl-Neelsen staining
BOB	Bacterial organ burden

Acknowledgements
Not applicable.

Authors' contributions
MYL, WKM, MW, LZ, and YHL conceived and designed the study and critically revised the manuscript. MYL, WKM, WM, WHZ, YB, HB, AB, RBC, ST, RZ, CGD, LZ and YHL performed animal experiments, dissections, and sampling, etc. MYL, WKM, WM and YLD conducted the laboratory experiments. All the authors read and approved the final manuscript.

Funding
This study was funded by the National Natural Science Foundation of Inner Mongolia (2022MS03023), Ordos Science & Technology Plan (YF20240007), First Class Discipline Research Special Project of Inner Mongolia Autonomous Region Department of Education (YLXKZX-NND-012), and Project of National Center of Technology Innovation for Dairy (2023-JSGG-5).

Data availability
No datasets were generated or analysed during the current study.

Declarations

Ethics approval and consent to participate
This study was performed in strict accordance with the international standards published in the Guide to the Feeding, Management and Use of Experimental Animals (8th Edition) and followed the Regulations on the Management of Experimental Animals and other relevant laws and regulations. The Biomedical Research Ethics Committee of Inner Mongolia Agricultural University approved this study (approval no. 2020 [078]). Additionally, during the experiment, we made all efforts to minimize animal suffering. We have obtained informed consent from all owners.

Consent for publication
Not applicable.

Competing Interest
The authors declare no competing interests.

Author details
[1]College of Veterinary Medicine, Inner Mongolia Agricultural University, Hohhot, China. [2]Key Laboratory of Clinical Diagnosis and Treatment Technology in Animal Disease, Ministry of Agriculture and Rural Affairs, Hohhot, China. [3]Animal Disease Control Center of Ordos, Ordos, China. [4]Otok Banner Animal Disease Prevention and Control Center, Ordos, China.

Received: 12 September 2024 Accepted: 17 April 2025
Published online: 29 April 2025

References

1. Fernández M, Delgado L, Sevilla IA, Fuertes M, Castaño P, Royo M, et al. Virulence attenuation of a Mycobacterium avium subspecies paratuberculosis S-type strain prepared from intestinal mucosa after bacterial culture. Evaluation in an experimental ovine model. Res Vet Sci. 2015;99:180–7. https://doi.org/10.1016/j.rvsc.2015.02.001.
2. Alonso-Hearn M, Molina E, Geijo M, Vazquez P, Sevilla I, Garrido JM, et al. Isolation of Mycobacterium avium subsp. paratuberculosis from muscle tissue of naturally infected cattle. Foodborne Pathog Dis. 2009;6(4):513–8. https://doi.org/10.1089/fpd.2008.0226.

3. Marquetoux N, Mitchell R, Ridler A, Heuer C, Wilson P. A synthesis of the patho-physiology of *Mycobacterium avium* subspecies *paratuberculosis* infection in sheep to inform mathematical modelling of ovine paratuberculosis. Vet Res. 2018;49(1):27. https://doi.org/10.1186/s13567-018-0522-1.
4. Whittington R, Donat K, Weber MF, Kelton D, Nielsen SS, Eisenberg S, et al. Control of paratuberculosis: who, why and how. A review of 48 countries. BMC Vet Res. 2019;15(1):198. https://doi.org/10.1186/s12917-019-1943-4.
5. Kuenstner JT, Naser S, Chamberlin W, Borody T, Graham DY, McNees A, et al. The consensus from the Mycobacterium avium ssp. paratuberculosis (MAP) conference 2017. Front Public Health. 2017;5:208. https://doi.org/10.3389/fpubh.2017.00208.
6. Galiero A, Fratini F, Mataragka A, Turchi B, Nuvoloni R, Ikonomopoulos J, et al. Detection of mycobacterium avium subsp. paratuberculosis in cheeses from small ruminants in Tuscany. Int J Food Microbiol. 2016;217:195–9. https://doi.org/10.1016/j.ijfoodmicro.2015.10.029.
7. Richardson H, Rhodes G, Henrys P, Sedda L, Weightman AJ, Pickup RW. Presence of *Mycobacterium avium* subspecies *paratuberculosis* monitored over varying temporal and spatial scales in river catchments: persistent routes for human exposure. Microorganisms. 2019;7(5): 136. https://doi.org/10.3390/microorganisms7050136.
8. Stevenson K, Hughes VM, de Juan L, Inglis NF, Wright F, Sharp JM. Molecular characterization of pigmented and nonpigmented isolates of Mycobacterium avium subsp. paratuberculosis. J Clin Microbiol. 2002;40(5):1798–804. https://doi.org/10.1128/JCM.40.5.1798-1804.2002.
9. Bryant JM, Thibault VC, Smith DG, McLuckie J, Heron I, Sevilla IA, et al. Phylogenomic exploration of the relationships between strains of *Mycobacterium avium* subspecies *paratuberculosis*. BMC Genomics. 2016;17:79. https://doi.org/10.1186/s12864-015-2234-5.
10. Mizzi R, Timms VJ, Price-Carter ML, Gautam M, Whittington R, Heuer C, et al. Comparative genomics of *Mycobacterium avium* subspecies *paratuberculosis* sheep strains. Front Vet Sci. 2021;8: 637637. https://doi.org/10.3389/fvets.2021.637637.
11. Zhao L, Wang Y, Wang JL, Zhao WH, Cheng HX, Ma YM, et al. Serological investigation and genotyping of Mycobacterium avium subsp. paratuberculosis in sheep and goats in Inner Mongolia, China. PLoS One. 2021;16(9): e0256628. https://doi.org/10.1371/journal.pone.0256628.
12. Sonawane GG, Narnaware SD, Tripathi BN. Molecular epidemiology of *Mycobacterium avium* subspecies *paratuberculosis* in ruminants in different parts of India. Int J Mycobacteriol. 2016;5(1):59–65. https://doi.org/10.1016/j.ijmyco.2015.11.003.
13. Hodgeman R, Mann R, Djitro N, Savin K, Rochfort S, Rodoni B. The pan-genome of Mycobacterium avium subsp. Paratuberculosis (Map) confirms ancestral lineage and reveals gene rearrangements within Map Type S. BMC Genomics. 2023;24(1):656. https://doi.org/10.1186/s12864-023-09752-0.
14. Fawzy A, Zschöck M, Ewers C, Eisenberg T. Genotyping methods and molecular epidemiology of Mycobacterium avium subsp. paratuberculosis (MAP). Int J Vet Sci Med. 2018;6(2):258–64. https://doi.org/10.1016/j.ijvsm.2018.08.001.
15. O'Brien R, Mackintosh CG, Bakker D, Kopecna M, Pavlik I, Griffin JFT. Immunological and molecular characterization of susceptibility in relationship to bacterial strain differences in Mycobacterium avium subsp. paratuberculosis infection in the red deer (Cervus elaphus). Infect Immun. 2006;74(6):3530–7. https://doi.org/10.1128/IAI.01688-05.
16. Stevenson K. Genetic diversity of *Mycobacterium avium* subspecies *paratuberculosis* and the influence of strain type on infection and pathogenesis: a review. Vet Res. 2015;46(1):64. https://doi.org/10.1186/s13567-015-0203-2.
17. Fernández M, Benavides J, Sevilla IA, Fuertes M, Castaño P, Delgado L, et al. Experimental infection of lambs with C and S-type strains of Mycobacterium avium subspecies paratuberculosis: immunological and pathological findings. Vet Res. 2014;45(1):5. https://doi.org/10.1186/1297-9716-45-5.
18. Stabel JR, Bannantine JP, Hostetter JM. Comparison of sheep, goats, and calves as infection models for Mycobacterium avium subsp. paratuberculosis. Vet Immunol Immunopathol. 2020;225: 110060. https://doi.org/10.1016/j.vetimm.2020.110060.
19. Stabel JR, Palmer MV, Harris B, Plattner B, Hostetter J, Robbe-Austerman S. Pathogenesis of Mycobacterium avium subsp. paratuberculosis in neonatal calves after oral or intraperitoneal experimental infection. Vet Microbiol. 2009;136(3–4):306–13. https://doi.org/10.1016/j.vetmic.2008.11.025.
20. Sweeney RW, Uzonna J, Whitlock RH, Habecker PL, Chilton P, Scott P. Tissue predilection sites and effect of dose on Mycobacterium avium subs. paratuberculosis organism recovery in a short-term bovine experimental oral infection model. Res Vet Sci. 2006;80(3):253–9. https://doi.org/10.1016/j.rvsc.2005.07.007.
21. Simutis FJ, Cheville NF, Jones DE. Investigation of antigen-specific T-cell responses and subcutaneous granuloma development during experimental sensitization of calves with *Mycobacterium avium* subsp *paratuberculosis*. Am J Vet Res. 2005;66(3):474–82. https://doi.org/10.2460/ajvr.2005.66.474.
22. Uzonna JE, Chilton P, Whitlock RH, Habecker PL, Scott P, Sweeney RW. Efficacy of commercial and field-strain Mycobacterium paratuberculosis vaccinations with recombinant IL-12 in a bovine experimental infection model. Vaccine. 2003;21(23):3101–9. https://doi.org/10.1016/s0264-410x(03)00261-5.
23. Waters WR, Miller JM, Palmer MV, Stabel JR, Jones DE, Koistinen KA, et al. Early induction of humoral and cellular immune responses during experimental Mycobacterium avium subsp. paratuberculosis infection of calves. Infect Immun. 2003;71(9):5130–8. https://doi.org/10.1128/IAI.71.9.5130-5138.2003.
24. Stabel JR, Palmer MV, Whitlock RH. Immune responses after oral inoculation of weanling bison or beef calves with a bison or cattle isolate of Mycobacterium avium subsp. paratuberculosis. J Wildl Dis. 2003;39(3):545–55. doi: 10.7589/0090-3558-39.3.545.
25. Williams ES, Snyder SP, Martin KL. Experimental infection of some North American wild ruminants and domestic sheep with *Mycobacterium paratuberculosis*: clinical and bacteriological findings. J Wildl Dis. 1983;19(3):185–91. https://doi.org/10.7589/0090-3558-19.3.185.
26. Rosseels V, Marché S, Roupie V, Govaerts M, Godfroid J, Walravens K, et al. Members of the 30-to 32-kilodalton mycolyl transferase family (Ag85) from culture filtrate of Mycobacterium avium subsp. paratuberculosis are immunodominant Th1-type antigens recognized early upon infection in mice and cattle. Infect Immun. 2006;74(1):202–12. https://doi.org/10.1128/IAI.74.1.202-212.2006.
27. Veazey RS, Horohov DW, Krahenbuhl JL, Taylor HW, Oliver JL 3rd, Snider TG 3rd. Comparison of the resistance of C57BL/6 and C3H/He mice to infection with *Mycobacterium paratuberculosis*. Vet Microbiol. 1995;47(1–2):79–87. https://doi.org/10.1016/0378-1135(95)00057-h.
28. Hamilton HL, Follett DM, Siegfried LM, Czuprynski CJ. Intestinal multiplication of *Mycobacterium paratuberculosis* in athymic nude gnotobiotic mice. Infect Immun. 1989;57(1):225–30. https://doi.org/10.1128/iai.57.1.225-230.1989.
29. Ghosh P, Shippy DC, Talaat AM. Superior protection elicited by live-attenuated vaccines in the murine model of paratuberculosis. Vaccine. 2015;33(51):7262–70. https://doi.org/10.1016/j.vaccine.2015.10.116.
30. Mokresh AH, Butler DG. Granulomatous enteritis following oral inoculation of newborn rabbits with *Mycobacterium paratuberculosis* of bovine origin. Can J Vet Res. 1990;54(3):313–9 PMID: 2379110.
31. Beard PM, Stevenson K, Pirie A, Rudge K, Buxton D, Rhind SM, et al. Experimental paratuberculosis in calves following inoculation with a rabbit isolate of Mycobacterium avium subsp. paratuberculosis. J Clin Microbiol. 2001;39(9):3080–4. https://doi.org/10.1128/JCM.39.9.3080-3084.2001.
32. Stuart P. Vaccination against Johne's disease in cattle exposed to experimental infection. Br Vet J. 1965;121(7):289–318. https://doi.org/10.1016/s0007-1935(17)41102-x.
33. Gilmour NJL, Angus KW, Mitchell B. Intestinal infection and host response to oral administration of *Mycobacterium johnei* in sheep. Vet Microbiol. 1977;2(3):223–35. https://doi.org/10.1016/0378-1135(77)90015-3.
34. Begara-Mcgorum I, Wildblood LA, Clarke CJ, Connor KM, Stevenson K, McInnes CJ, et al. Early immunopathological events in experimental ovine paratuberculosis. Vet Immunol Immunopathol. 1998;63(3):265–87. https://doi.org/10.1016/s0165-2427(98)00107-x.
35. Beard PM, Rhind SM, Sinclair MC, Wildblood LA, Stevenson K, McKendrick IJ, et al. Modulation of gammadelta T cells and CD1 in Mycobacterium avium subsp. paratuberculosis infection. Vet Immunol

Immunopathol. 2000;77(3–4):311–9. https://doi.org/10.1016/s0165-2427(00)00238-5.
36. Hirch A. Infection of hamsters and rabbits with *Mycobacterium johnei*. J Comp Pathol. 1956;66(3):260–9. https://doi.org/10.1016/s0368-1742(56)80027-1.
37. Koo HC, Park YH, Ahn J, Waters WR, Hamilton MJ, Barrington G, et al. New latex bead agglutination assay for differential diagnosis of cattle infected with Mycobacterium bovis and Mycobacterium avium subsp. paratuberculosis. Clin Diagn Lab Immunol. 2004;11(6):1070–74. doi: 10.1128/CDLI.11.6.1070-1074.2004.
38. Lee JH, Park H-T, Shim S, Kim S, Woo S-H, Kim D-Y, et al. Immunopathological mechanisms in the early stage of Mycobacterium avium subsp. paratuberculosis infection via different administration routes in a murine model. PloS One. 2023;18(2): e0281880. https://doi.org/10.1371/journal.pone.0281880.
39. Purdie AC, Plain KM, Pooley H, Begg DJ, de Silva K, Whittington RJ. Correlates of vaccine protection against *Mycobacterium avium* subspecies *paratuberculosis* infection revealed in a transcriptomic study of responses in Gudair® vaccinated sheep. Front Vet Sci. 2022;9: 1004237. https://doi.org/10.3389/fvets.2022.1004237.
40. Begg DJ, de Silva K, Fiore LD, Taylor DL, Bower K, Zhong L, et al. Experimental infection model for Johne's disease using a lyophilised, pure culture, seedstock of *Mycobacterium avium* subspecies *paratuberculosis*. Vet Microbiol. 2010;141(3–4):301–11. https://doi.org/10.1016/j.vetmic.2009.09.007.
41. Reddacliff LA, Whittington RJ. Experimental infection of weaner sheep with S strain Mycobacterium avium subsp. paratuberculosis. Vet Microbiol. 2003;96(3):247–58. https://doi.org/10.1016/j.vetmic.2003.07.004.
42. Reddacliff LA, Nicholls PJ, Vadali A, Whittington RJ. Use of growth indices from radiometric culture for quantification of sheep strains of Mycobacterium avium subsp. paratuberculosis. Appl Environ Microbiol. 2003;69(6):3510–6. https://doi.org/10.1128/AEM.69.6.3510-3516.2003.
43. Stewart DJ, Vaughan JA, Stiles PL, Noske P, Tizard MLV, Prowse SJ, et al. A long-term study in Angora goats experimentally infected with Mycobacterium avium subsp. paratuberculosis: clinical disease, faecal culture and immunological studies. Vet Microbiol. 2006;113(1–2):13–24. https://doi.org/10.1016/j.vetmic.2005.09.015.
44. Lepper AW, Wilks CR, Kotiw M, Whitehead JT, Swart KS. Sequential bacteriological observations in relation to cell-mediated and humoral antibody responses of cattle infected with *Mycobacterium paratuberculosis* and maintained on normal or high iron intake. Aust Vet J. 1989;66(2):50–5. https://doi.org/10.1111/j.1751-0813.1989.tb03015.x.
45. Begg DJ, Plain KM, de Silva K, Gurung R, Gunn A, Purdie AC, et al. Immunopathological changes and apparent recovery from infection revealed in cattle in an experimental model of Johne's disease using a lyophilised culture of *Mycobacterium avium* subspecies *paratuberculosis*. Vet Microbiol. 2018;219:53–62. https://doi.org/10.1016/j.vetmic.2018.03.029.
46. Vaughan JA, Lenghaus C, Stewart DJ, Tizard ML, Michalski WP. Development of a Johne's disease infection model in laboratory rabbits following oral administration of *Mycobacterium avium* subspecies *paratuberculosis*. Vet Microbiol. 2005;105(3–4):207–13. https://doi.org/10.1016/j.vetmic.2004.10.019.
47. Fernández B, Colavecchia SB, Ingratta GG, Jolly A, Stempler A, Fortuny ML, et al. Early IgG2 in calves experimentally infected with Mycobacterium avium subsp. paratuberculosis. Vet Immunol Immunopathol. 2019;213: 109886. https://doi.org/10.1016/j.vetimm.2019.109886.
48. Ingratta GG, Stempler A, Fernández B, Colavecchia SB, Jolly A, Minatel L, et al. Early-stage findings in an experimental calf model infected with Argentinean isolates of Mycobacterium avium subsp. paratuberculosis. Vet Immunol Immunopathol. 2023;259: 110595. https://doi.org/10.1016/j.vetimm.2023.110595.
49. Colavecchia SB, Fernández B, Jolly A, Minatel L, Hajos SE, Paolicchi FA, et al. Immunological findings associated with Argentinean strains of Mycobacterium avium subsp. paratuberculosis in bovine models. Vet Immunol Immunopathol. 2016;176:28–33. https://doi.org/10.1016/j.vetimm.2016.04.010.
50. Olivieri MAC, Cuerda MX, Moyano RD, Gravisaco MJ, Pinedo MFA, Delgado FO, et al. Superior protection against paratuberculosis by a heterologous prime-boost immunization in a murine model. Vaccine. 2024;15:S0264-410X(24), 00696–0. https://doi.org/10.1016/j.vaccine.2024.06.022.
51. Olivieri MAC, Moyano RD, Traveria GE, Pinedo MFA, Mon ML, Gravisaco MJ, et al. Protection efficacy of Argentinian isolates of Mycobacterium avium subsp. paratuberculosis with different genotypes and virulence in a murine model. Res Vet Sci. 2018;121:4–11. https://doi.org/10.1016/j.rvsc.2018.09.009.
52. Corbett CS, Barkema HW, De Buck J. Quantifying fecal shedding of Mycobacterium avium ssp. paratuberculosis from calves after experimental infection and exposure. J Dairy Sci. 2018;101(2):1478–87. https://doi.org/10.3168/jds.2017-13544.
53. Stinson KJ, Duffield TF, Kelton DF, Baquero MM, Plattner BL. A preliminary study investigating effects of oral monensin sodium in an enteric Mycobacterium avium ssp. paratuberculosis infection model of calves. J Dairy Sci. 2019;102(10):9097–106. https://doi.org/10.3168/jds.2018-15980.
54. Dukes TW, Glover GJ, Brooks BW, Duncan JR, Swendrowski M. Paratuberculosis in saiga antelope (*Saiga tatarica*) and experimental transmission to domestic sheep. J Wildl Dis. 1992;28(2):161–70. https://doi.org/10.7589/0090-3558-28.2.161.
55. Eshraghisamani R, Arrazuria R, Luo L,De Buck J. Evaluation of *Mycobacterium avium* subsp. *paratuberculosis* isocitrate lyase (IcL) and ABC transporter (BacA) knockout mutants as vaccine candidates. Front Cell Infect Microbiol. 2023;13:1149419. https://doi.org/10.3389/fcimb.2023.1149419.
56. Duffy SC, Lupien A, Elhaji Y, Farag M, Marcus V, Behr MA. Establishment of persistent enteric mycobacterial infection following streptomycin pre-treatment. Gut Pathog. 2023;15(1):46. https://doi.org/10.1186/s13099-023-00573-w.
57. Arrazuria R, Elguezabal N, Juste RA, Derakhshani H, Khafipour E. *Mycobacterium avium* subspecies *paratuberculosis* infection modifies gut microbiota under different dietary conditions in a rabbit model. Front Microbiol. 2016;7:446. https://doi.org/10.3389/fmicb.2016.00446.
58. Gwozdz JM, Thompson KG, Manktelow BW, Murray A, West DM. Vaccination against paratuberculosis of lambs already infected experimentally with *Mycobacterium avium* subspecies *paratuberculosis*. Aust Vet J. 2000;78(8):560–6. https://doi.org/10.1111/j.1751-0813.2000.tb11902.x.
59. Begg DJ, O'brien R, Mackintosh CG, Griffin JFT. Experimental infection model for Johne's disease in sheep. Infect Immun. 2005;73(9):5603–11. https://doi.org/10.1128/IAI.73.9.5603-5611.2005.
60. Dukkipati VSR, Ridler AL, Thompson KG, Buddle BM, Hedgespeth BA, Price-Carter M, et al. Experimental infection of New Zealand Merino sheep with a suspension of *Mycobacterium avium* subspecies *paratuberculosis* (Map) strain Telford: kinetics of the immune response, histopathology and Map culture. Vet Microbiol. 2016;195:136–43. https://doi.org/10.1016/j.vetmic.2016.09.018.
61. Juste RA, Marín JFG, Peris B, de Ocáriz CSS, Badiola JJ. Experimental infection of vaccinated and non-vaccinated lambs with *Mycobacterium paratuberculosis*. J Comp Pathol. 1994;110(2):185–94. https://doi.org/10.1016/s0021-9975(08)80189-2.
62. Verna AE, Garcia-Pariente C, Muñoz M, Moreno O, García-Marin JF, Romano MI, et al. Variation in the immuno-pathological responses of lambs after experimental infection with different strains of Mycobacterium avium subsp. paratuberculosis. Zoonoses Public Health. 2007;54(6–7):243–52. https://doi.org/10.1111/j.1863-2378.2007.01058.x.
63. Delgado L, García Marín JF, Muñoz M, Benavides J, Juste RA, García-Pariente C, et al. Pathological findings in young and adult sheep following experimental infection with 2 different doses of *Mycobacterium avium* Subspecies *paratuberculosis*. Vet Pathol. 2013;50(5):857–66. https://doi.org/10.1177/0300985813476066.
64. Arteche-Villasol N, Gutiérrez-Expósito D, Criado M, Benavides J, Pérez V. Assessment of paratuberculosis vaccination effect on in vitro formation of neutrophil extracellular traps in a sheep model. Vaccines (Basel). 2022;10(9): 1403. https://doi.org/10.3390/vaccines10091403.
65. Arrazuria R, Molina E, Mateo-Abad M, Arostegui I, Garrido JM, Juste RA, et al. Effect of various dietary regimens on oral challenge with Mycobacterium avium subsp. paratuberculosis in a rabbit model. Res Vet Sci. 2015;101:80–3. https://doi.org/10.1016/j.rvsc.2015.06.006.
66. Arrazuria R, Molina E, Garrido JM, Pérez V, Juste RA, Elguezabal N. Vaccination sequence effects on immunological response and tissue

bacterial burden in paratuberculosis infection in a rabbit model. Vet Res. 2016;47(1):77. https://doi.org/10.1186/s13567-016-0360-y.
67. Ladero-Auñon I, Molina E, Oyanguren M, Barriales D, Fuertes M, Sevilla IA, et al. Oral vaccination stimulates neutrophil functionality and exerts protection in a Mycobacterium avium subsp. paratuberculosis infection model. NPJ Vaccines. 2021;6(1):102. https://doi.org/10.1038/s41541-021-00367-8.
68. Köhler H, Soschinka A, Meyer M, Kather A, Reinhold P, Liebler-Tenorio E. Characterization of a caprine model for the subclinical initial phase of Mycobacterium avium subsp. paratuberculosis infection. BMC Vet Res. 2015;11:74. https://doi.org/10.1186/s12917-015-0381-1.
69. Krüger C, Köhler H, Liebler-Tenorio EM. Sequential development of lesions 3, 6, 9, and 12 months after experimental infection of goat kids with *Mycobacterium avium* subsp *paratuberculosis*. Vet Pathol. 2015;52(2):276–90. https://doi.org/10.1177/0300985814533804.
70. Klausen J, Pérez V, Giese SB, García Marín JF, Ahrens P. Immunological detection of sheep experimentally infected with strains of *Mycobacterium avium* subspecies containing insertion sequence IS901/IS902 and a 40 kDa protein. Vet Microbiol. 1997;57(2–3):181–7. https://doi.org/10.1016/s0378-1135(97)00133-8.
71. Tanaka S, Itohara S, Sato M, Taniguchi T, Yokomizo Y. Reduced formation of granulomata in γδ T cell knockout BALB/c mice inoculated with Mycobacterium avium subsp. paratuberculosis. Vet Pathol. 2000;37(5):415–21. https://doi.org/10.1354/vp.37-5-415.
72. Krishnappa G, Jagannath C, Rao BU. The specificity of antibody response in experimental and natural bovine paratuberculosis studied by crossed immunoelectrophoresis with intermediate gel. Vet Microbiol. 1989;21(1):67–78. https://doi.org/10.1016/0378-1135(89)90019-9.
73. Kurade NP, Tripathi BN, Rajukumar K, Parihar NS. Sequential development of histologic lesions and their relationship with bacterial isolation, fecal shedding, and immune responses during progressive stages of experimental infection of lambs with Mycobacterium avium subsp. paratuberculosis. Vet Pathol. 2004;41(4):378–87. https://doi.org/10.1354/vp.41-4-378.
74. Begum J, Das P, Lingaraju MC. Molecular and histopathological evaluation of the efficacy of saponified and Freund's incomplete adjuvanted paratuberculosis killed vaccine in murine model. Indian J Anim Res. 2017;51(3):510–7. https://doi.org/10.18805/ijar.v0iOF.7602.
75. Haghkhah M, Hemati Z, Derakhshandeh A, Namazi F, Chaubey KK, Singh SV. Immuno-reactivity evaluation of Mce-truncated subunit candidate vaccine against *Mycobacterium avium* subspecies *paratuberculosis* challenge in the goat models. BMC Vet Res. 2023;19(1):157. https://doi.org/10.1186/s12917-023-03715-z.
76. Robbers L, van de Mheen R, Benedictus L, Jorritsma R, Nielen M, Bijkerk HJC, et al. Evidence for transfer of maternal antigen specific cellular immunity against Mycobacterium avium ssp. paratuberculosis via colostrum in a goat twin model. Vet Immunol Immunopathol. 2022;246: 110402. https://doi.org/10.1016/j.vetimm.2022.110402.
77. Pagliasso G, Blasio AD, Vitale N, Romano A, Decastelli L, Quasso A, et al. Goat paratuberculosis: experimental model for the evaluation of *Mycobacterium* persistence in raw milk cheese. Microorganisms. 2021;9(10):2032. https://doi.org/10.3390/microorganisms9102032.
78. Yu Y, Zhang S, Xu G, Xu D, Zheng H, Li B, et al. Identification of *Mycobacterium avium* subspecies *paratuberculosis* in sheep farms in Bayannaoer, Inner Mongolia, China. BMC Vet Res. 2022;18(1):281. https://doi.org/10.1186/s12917-022-03293-6.
79. Marchesi JR, Sato T, Weightman AJ, Martin TA, Fry JC, Hiom SJ, et al. Design and evaluation of useful bacterium-specific PCR primers that amplify genes coding for bacterial 16S rRNA. Appl Environ Microbiol. 1998;64(2):795–9. https://doi.org/10.1128/AEM.64.2.795-799.1998.
80. Alonso-Hearn M, Ballesteros A, Navarro A, Badia-Bringué G, Casais R. Lateral-flow assays for bovine paratuberculosis diagnosis. Front Vet Sci. 2023;10: 1257488. https://doi.org/10.3389/fvets.2023.1257488.
81. Idris SM, Eltom KH, Okuni JB, Ojok L, Elmagzoub WA, El Wahed AA, et al. Paratuberculosis: the hidden killer of small ruminants. Animals. 2021;12(1): 12. https://doi.org/10.3390/ani12010012.
82. Yue R, Liu C, Barrow P, Liu F, Cui Y, Yang L, et al. The isolation and molecular characterization of Mycobacterium avium subsp. paratuberculosis in Shandong province, China. Gut Pathog. 2016;8(1):9. https://doi.org/10.1186/s13099-016-0092-6.
83. Jolly A, Fernández B, Mundo SL, Elguezabal N. Modeling paratuberculosis in laboratory animals, cells, or tissues: a focus on their applications for pathogenesis, diagnosis, vaccines, and therapy studies. Animals. 2023;13(22): 3553. https://doi.org/10.3390/ani13223553.
84. Yang J, Lv Y, Zhu Y, Li S, Tao J, Chang L, et al. Baseline T-lymphocyte and cytokine indices in sheep peripheral blood. BMC Vet Res. 2022;18(1):165. https://doi.org/10.1186/s12917-022-03268-7.
85. Behr MA, Collins DM. Paratuberculosis: organism, disease, control. CABI. 2022.
86. Roberto JPL, Limeira CH, Araújo Júnior JP, Malossi CD, Ullmann LS, Silva MLCR, et al. Clinical, histopathological, and molecular findings for *Mycobacterium avium* subspecies *paratuberculosis* (MAP) in dairy goats under semiarid conditions. Tuberculosis (Edinb). 2023;139: 102319. https://doi.org/10.1016/j.tube.2023.102319.
87. Whittington RJ, Sergeant ES. Progress towards understanding the spread, detection and control of *Mycobacterium avium* subsp *paratuberculosis* in animal populations. Aust Vet J. 2001;79(4):267–78. https://doi.org/10.1111/j.1751-0813.2001.tb11980.x.
88. Hines ME 2nd, Stabel JR, Sweeney RW, Griffin F, Talaat AM, Bakker D, et al. Experimental challenge models for Johne's disease: a review and proposed international guidelines. Vet Microbiol. 2007;122(3–4):197–222. https://doi.org/10.1016/j.vetmic.2007.03.009.
89. Stewart DJ, Vaughan JA, Stiles PL, Noske PJ, Tizard ML, Prowse SJ, et al. A long-term study in Merino sheep experimentally infected with Mycobacterium avium subsp. paratuberculosis: clinical disease, faecal culture and immunological studies. Vet Microbiol. 2004;104(3–4):165–78. https://doi.org/10.1016/j.vetmic.2004.09.007.
90. Kawaji S, Begg DJ, Plain KM, Whittington RJ. A longitudinal study to evaluate the diagnostic potential of a direct faecal quantitative PCR test for Johne's disease in sheep. Vet Microbiol. 2011;148(1):35–44. https://doi.org/10.1016/j.vetmic.2010.07.022.
91. Bruczyńska M, Didkowska A, Brzezińska S, Nowak M, Filip-Hutsch K, Kalicki M, et al. *Mycobacterium avium* subspecies *paratuberculosis* in asymptomatic zoo herbivores in Poland. Animals. 2023;13(6): 1022. https://doi.org/10.3390/ani13061022.
92. Stewart DJ, Vaughan JA, Stiles PL, Noske PJ, Jones SL. A long-term study in Angora goats experimentally infected with Mycobacterium avium subsp. paratuberculosis: clinical disease, faecal culture and immunological studies. Vet Microbiol. 2006;104(3–4):165–78. https://doi.org/10.1016/j.vetmic.2005.09.015.
93. Hodgeman R, Liu Y, Rochfort S, Rodoni B. Development and evaluation of genomics informed real-time PCR assays for the detection and strain typing of Mycobacterium avium subsp. paratuberculosis. J Appl Microbiol. 2024;135(5):lxae107. https://doi.org/10.1093/jambio/lxae107.
94. Preziuso S, Magi GE, Renzoni G. Detection of Mycobacterium avium subsp. paratuberculosis in intestinal and mammary tissues and in lymph nodes of sheep with different techniques and its relationship with enteric lesions. Small Ruminant Res. 2012;105(1–3):295–9. https://doi.org/10.1016/j.smallrumres.2011.11.015.
95. Delgado L, Juste RA, Muñoz M, Morales S, Benavides J, Ferreras MC, et al. Differences in the peripheral immune response between lambs and adult ewes experimentally infected with *Mycobacterium avium* subspecies *paratuberculosis*. Vet Immunol Immunopathol. 2012;145(1–2):23–31. https://doi.org/10.1016/j.vetimm.2011.10.005.
96. Salgado M, Kruze J, Collins MT. Diagnosis of paratuberculosis by fecal culture and ELISA on milk and serum samples in two types of Chilean dairy goat herds. J Vet Diagn Invest. 2007;19:99–102. https://doi.org/10.1177/104063870701900117.
97. Konieczny K, Pomorska-Mól M. A literature review of selected bacterial diseases in alpacas and llamas—epidemiology, clinical signs and diagnostics. Animals. 2023;14(1): 45. https://doi.org/10.3390/ani14010045.
98. de Silva K, Begg D, Whittington R. The interleukin 10 response in ovine Johne's disease. Vet Immunol Immunopathol. 2011;139:10–6. https://doi.org/10.1016/j.vetimm.
99. Coussens PM, Verman N, Coussens MA, Elftman MD, McNulty AM. Cytokine gene expression in peripheral blood mononuclear cells and tissues of cattle infected with Mycobacterium avium subsp. paratuberculosis: evidence for an inherent proinflammatory gene expression pattern. Infect Immunity. 2004;72:1409–22. https://doi.org/10.1128/iai.72.3.1409-1422.2004.

100. De Silva K, Begg DJ, Plain KM, Purdie AC, Kawaji S, Dhand NK, et al. Can early host responses to mycobacterial infection predict eventual disease outcomes? Prev Vet Med. 2013;112(3–4):203–12. https://doi.org/10.1016/j.prevetmed.2013.08.006.
101. Verin R, Perroni M, Rossi G, De Grossi L, Botta R, De Sanctis B, et al. Paratuberculosis in sheep: histochemical, immunohistochemical and in situ hybridization evidence of in utero and milk transmission. Res Vet Sci. 2016;106:173–9. https://doi.org/10.1016/j.rvsc.2016.04.006.
102. Anwar SI, Gharieb SA. Detection of subclinical paratuberculosis in dairy cattle in Egypt. Iraqi J Vet Scis. 2024;38(1):139–46. https://doi.org/10.33899/IJVS.2023.141286.3110.
103. Pérez V, Marín JFG, Badiola JJ. Description and classification of different types of lesion associated with natural paratuberculosis infection in sheep. J Comp Pathol. 1996;114(2):107–22. https://doi.org/10.1016/s0021-9975(96)80001-6.
104. Dennis MM, Reddacliff LA, Whittington RJ. Longitudinal study of clinicopathological features of Johne's disease in sheep naturally exposed to *Mycobacterium avium* subspecies *paratuberculosis*. Vet Pathol. 2011;48(3):565–75. https://doi.org/10.1177/0300985810375049.
105. Scherrer S, Stephan R, Zumthor JP, Kipar A, Seehusen F. Morphological and molecular characterization of a new Mycobacterium avium subsp. paratuberculosis S-type strain genotype in goats. Front Vet Sci. 2019;6:250. https://doi.org/10.3389/fvets.2019.00250.
106. González J, Geijo M, García-Pariente C, Verna A, Corpa J, Reyes L, et al. Histopathological classification of lesions associated with natural paratuberculosis infection in cattle. J Comp Pathol. 2005;133(2–3):184–96. https://doi.org/10.1016/j.jcpa.2005.04.007.
107. Koets AP, Eda S, Sreevatsan S. The within host dynamics of *Mycobacterium avium* ssp *paratuberculosis* infection in cattle: where time and place matter. Vet Res. 2015;46(1):61. https://doi.org/10.1186/s13567-015-0185-0.

Publisher's Note